



NIH PUBLIC ACCESS

Author Manuscript

J Innov Opt Health Sci. Author manuscript; available in PMC 2009 November 25.

Published in final edited form as:

J Innov Opt Health Sci. 2008 October 1; 1(2): 207–215. doi:10.1142/S1793545808000212.

Simultaneous imaging of a lacZ-marked tumor and microvasculature morphology *in vivo* by dual-wavelength photoacoustic microscopy

Li Li^{*}, Hao F. Zhang^{*,†}, Roger J. Zemp^{*,‡}, Konstantin Maslov^{*}, and Lihong Wang^{*,§}^{*} Optical Imaging Laboratory, Department of Biomedical Engineering, Washington University in St. Louis, St. Louis, Missouri, USA 63130[†] Now with Department of Electrical Engineering, University of Wisconsin-Milwaukee, Milwaukee, Wisconsin, USA 53201[‡] Now with Department of Electrical and Computer Engineering, University of Alberta, Edmonton, Alberta, Canada T6G2V4

Abstract

Photoacoustic molecular imaging, combined with the reporter-gene technique, can provide a valuable tool for cancer research. The expression of the lacZ reporter gene can be imaged using photoacoustic imaging following the injection of X-gal, a colorimetric assay for the lacZ-encoded enzyme β -galactosidase. Dual-wavelength photoacoustic microscopy was used to non-invasively image the detailed morphology of a lacZ-marked 9L gliosarcoma and its surrounding microvasculature simultaneously *in vivo*, with a superior resolution on the order of 10 μ m. Tumor-feeding vessels were found, and the expression level of lacZ in tumor was estimated. With future development of new absorption-enhancing reporter-gene systems, we anticipate this strategy can lead to a better understanding of the role of tumor metabolism in cancer initiation, progression, and metastasis, and in its response to therapy.

Keywords

photoacoustic; molecular imaging; gene expression; reporter gene

Cancer is a major threat to public health around the world. In the US, it accounts for ~23% of total deaths, second only to the heart disease. In 2007, it was reported that ~1.44 million new cancer cases were diagnosed, while ~0.56 million people died from it.¹ Although we have fought against cancer for centuries, our knowledge of its fundamental mechanisms is still incomplete. In the past decade, advances in genetics and molecular cell biology have opened a new window for us to understand the molecular bases of cancer. However, this progress has mainly come from studies of cultured cells or excised tissue. Researchers can achieve only a single data point from each culture or animal. Therefore, it is typically a time-consuming and labor-intensive task to completely investigate the role of a single gene or protein in a specific pathway. Furthermore, information obtained in a simplified environment *in vitro* may not correlate with what happens *in vivo*.

Recently, molecular imaging, although still in its infancy, has emerged as a promising tool to meet these challenges.² Molecular imaging marries state-of-the-art imaging modalities with

§Corresponding author. lhwang@biomed.wustl.edu.

modern biochemistry, which makes molecular probes that target specific molecules of interest and provide corresponding imaging contrast. As a result of its non-invasive nature, molecular imaging allows biologists to see molecule-specific events in a desired spatial-temporal order in their native environment in living small-animal models. The required manpower and resources are significantly reduced. The great potential of molecular imaging in cancer research has been shown by various pioneering applications in studies of cancer initiation, progression, and response to therapy.³ In this paper, we present our current progress in developing a new paradigm of molecular imaging, which combines photoacoustic imaging and the reporter gene technique.

Our method falls into an important branch of molecular imaging, which provides an insight into molecular mechanisms by locating and quantifying the expression of a special reporter gene.⁴ A reporter gene is a short segment of extragenous DNA, whose protein product (the molecular probe) can be visualized by an imaging tool either directly or by acting on an analyzing assay. The reporter gene technique has versatile applications in cancer research. For example, a reporter gene can be incorporated into the genome of a tumor under the control of a strong promoter to serve as an *in-vivo* mark for tracking tumor appearance, growth, and metastasis.⁵ Also, it is generally believed that nearly all cancers involve genetic abnormality. When fused to regulatory regions of a gene of interest, the expression level of the reporter gene reveals the different regulations of the targeted gene during different stages of cancer development.⁶ In addition, reporter-gene imaging can significantly accelerate the development process of new cancer treatment, particularly the gene therapy. By coordinately expressing a reporter gene and the therapeutic gene, molecular imaging will allow us to monitor the delivery, targeting, expression, and regulation of the therapeutic gene *in vivo*, and greatly facilitate our rational optimization of the treatment strategy.⁷

Photoacoustic imaging is a new non-invasive optical imaging modality, which uniquely exploits optical-absorption contrast.⁸ By utilizing laser-induced ultrasound, it is not limited by strong optical scattering in biological tissue, and thus overcomes the resolution obstacle to deep imaging existing in pure optical techniques. In a word, photoacoustic imaging combines the most appealing features of both optics and ultrasonics: high optical absorption contrast and sub-mm ultrasonic resolution. As a result, photoacoustic imaging has rapidly emerged as a powerful tool for small animal imaging in the past few years.^{9,10,11} It is specially attractive for cancer researchers, because it is the only technique to date that can provide functional information about local metabolism in opaque tissue, such as tumor angiogenesis¹², total hemoglobin concentration and saturation level of oxygen^{13,14}, and potentially the local oxygen metabolic rate, using endogenous contrast. It is generally believed that tumor angiogenesis and local metabolism change play key roles in tumor growth and metastasis.¹⁵

As the initial step in our efforts to develop photoacoustic molecular imaging for -studying tumor pathology, we employ a widely-used reporter-gene technique based on lacZ¹⁶. The lacZ reporter gene encodes β -galactosidase, an E. coli enzyme responsible for lactose metabolism. We use a sensitive colorimetric assay, 5-bromo-4-chloro-3-indolyl- β -D-galactoside (X-gal), for β -galactosidase staining. X-gal is an optically transparent lactose-like substrate for β -galactosidase. After X-gal's glycosidic linkage is cleaved by β -galactosidase, a stable dark blue product is produced. The dark product has a strong absorption in the red region of the optical spectrum, and gives an excellent target for photoacoustic imaging. The lacZ technique possesses two noticeable advantages. First, β -galactosidase and X-gal alone are colorless. Strong optical absorption, which photoacoustic imaging is sensitive to, is generated only when they co-exist. Imaging β -galactosidase with photoacoustic imaging does not require complete clearance of the extra un-cleaved X-gal. Second, the lacZ technique possesses an intrinsic signal-amplification mechanism. As an enzyme, a single β -galactosidase molecule can cleave multiple X-gal molecules to produce a large number of blue product molecules, allowing us

to detect a low expression level of lacZ. In an earlier report, we have proved the feasibility of visualizing the lacZ gene expression using a circular-scanning photoacoustic tomographic system.¹⁶ However, the spatial resolution was not adequate to map the surrounding microvasculature, a considerable benefit of photoacoustic molecular imaging.

To achieve better resolution, we have employed a new technique: dual-wavelength reflection-mode photoacoustic microscopy¹⁷ (Fig. 1). A tunable dye laser (ND6000, Continuum), pumped by a Q-switched Nd:YAG laser (Brilliant, Bigsky), provided laser pulses at two different wavelengths, 584 nm and 635 nm. Each laser pulse had a duration of 6.5 ns, and a pulse repetition rate of 10 Hz. The laser output was delivered to the imaging system through a multimode fiber with a 600- μm core diameter. The components in the dashed rectangle in Fig. 1 were assembled as a scanning probe. The light coming out of the fiber was first expanded by a conical lens to form an annular beam and then weakly focused into the tissue, with its focal region coaxially overlapping the focus of a high-frequency ultrasonic transducer (V214-BCRM, Panametrics). The incident energy density at the tissue surface was controlled to be under 6 mJ/cm^2 , which was well within the ANSI safety standards.¹⁸ By using dark-field illumination with an incident angle of 45° , the strong acoustic waves otherwise emitted from structures close to the skin were reduced, which allowed us to image deeper structures better. The transducer had a central frequency of 50 MHz, a nominal bandwidth of 70%, and an NA of 0.44. It was immersed in water inside a tank with an opening at the bottom that was sealed with a thin transparent plastic membrane. The animal was placed below the membrane outside the tank. Ultrasound gel was applied on the chemically depilated skin for better acoustic coupling. The photoacoustic signal received by the transducer was amplified and then recorded by a digital oscilloscope (sampling rate: 250 MHz). At each lateral position, the data acquisition lasted for 2 μs , without averaging. A mechanical stage drove the raster scanning of the imaging probe to obtain a volumetric dataset. The acquired data was first processed by a synthetic-aperture focusing technique¹⁹ to correct for the blurring outside the ultrasonic focus. The maximum photoacoustic amplitudes along each axial line were then projected on the skin surface, to form a maximum-amplitude projection (MAP) image. In previous experiments, the current system was quantified to have a lateral resolution of 45 μm and an axial resolution of 15 μm , and was capable of imaging $\sim 3 \text{ mm}$ deep into the skin.¹¹ In addition, the resolution scales with the transducer's bandwidth, and can be further improved by employing a transducer with a broader bandwidth, at the cost of imaging depth.

The two wavelengths (584 nm and 635 nm) were chosen to maximize the difference between the optical absorption of hemoglobin and the blue product within the efficient emission range of the laser dye. We quantitatively measured the molar extinction spectrum of the blue product¹⁶, and compare it in Fig. 2 with the documented absorption spectrum of two major forms of hemoglobin²⁰, oxyhemoglobin (HbO_2) and deoxyhemoglobin (HbR). The 584-nm wavelength was used to visualize the microvasculature. It is an isosbestic spectral point of hemoglobin, where HbO_2 and HbR have identical molar extinction coefficients, which dominate that of the blue product by a 5.4:1 ratio. The photoacoustic amplitude in the image acquired at 584 nm directly correlate with the local total hemoglobin concentration. The 635-nm wavelength was selected to map the lacZ-marked tumor, where the molar extinction coefficient of the blue product was 20.4 times greater than HbO_2 's and 2.2 times greater than HbR 's. Although this difference becomes bigger at longer wavelengths, the laser output was strongest at 635 nm.

Five million 9L/LacZ gliosarcoma tumor cells (ATCC) were implanted under the scalps of Sprague-Dawley rats (80–100 g, Harlan). Gliosarcoma is a malignant neoplasm of the central nervous system. Unlike other cerebral gliomas, gliosarcoma has a propensity for extracranial metastasis through the vascular pathway.²¹ After the presence of the tumor was noticeable, 20 μl of X-gal solution (20 mg/ml, Fermentas) was injected near the tumor one day before PAM

imaging. During the experiment, the animals were kept under anesthesia using isoflurane gas. The heart rate and the global arterial blood oxygenation were closely monitored using a pulse oximeter (8600, Nonin Medical), while the body temperature of the animal was maintained at 36°C.

The lacZ-marked 9L gliosarcoma was clearly visualized in the photoacoustic image acquired at 635 nm [Fig. 3(A)]. Our previous study¹⁶ also showed that, unlike a strongly absorbing melanoma¹⁷, the 9L gliosarcoma did not show up in photoacoustic images without X-gal staining. This implied that the reporter-gene technique is important in developing photoacoustic molecular imaging for studying most “invisible” tumors. In addition, the non-tumor region at a similar anatomical position also did not manifest in the photoacoustic images after the injection of X-gal, proving that no significant amount of endogenous β -galactosidase existed. The strong photoacoustic signal in Fig. 3(B) did come from the X-gal-stained tumor with the lacZ tag. Furthermore, the morphology of the surrounding microvasculature was mapped in great details in the MAP image taken at 584 nm [Fig. 3(B)]. The photoacoustic signal in Fig. 3(B) represents the relative value of total hemoglobin concentration, a key parameter of local metabolism. A combined pseudo-colored image [Fig. 3(C)] shows the spatial relation between the tumor and the surrounding microvasculature. From it, we were able to identify several tumor feeding vessels, which are indicated by arrows in Fig. 3.

We were also able to assess the expression level of lacZ in the tumor. Under the assumption of uniform local optical fluence, the amplitude of the photoacoustic image is linearly proportional to the local absorption coefficient⁸, which is the product of molecule's concentration and its molar extinction coefficient. In Fig. 3(A), the photoacoustic amplitudes from the lacZ-marked tumor and the residual blood vessels were estimated to have a 4.0:1 ratio. From the literature, the concentration of hemoglobins in normal blood is about 2.3 mM.²⁰ Assuming blood has an oxygen saturation level of 90% and taking into account the aforementioned relations among molar extinction coefficients, we estimated the concentration of the blue cleavage product to be $\sim 840 \mu\text{M}$ in the tumor. Given efficient delivery of X-gal, this estimated concentration of blue product will positively correlate with the concentration of β -galactosidase, i.e., the expression level of lacZ gene. Also, the tumor image in Fig. 3(A) had low background, excluding the residual blood vessels. We estimated that the stained tumor was imaged with a signal-to-noise ratio (SNR) of ~ 36.6 dB. Hence, the minimum detectable concentration of blue product (with SNR=1) was less than $12.3 \mu\text{M}$. The detection threshold of the real expression product, β -galactosidase, was expected to be several orders of magnitude lower than this value. Hence, the sensitivity of our strategy fell between those of magnetic resonance imaging (sub-mM) and fluorescence imaging (100 fM).

Compared to our previous work, the current strategy using dual-wavelength photoacoustic microscopy made progress in three aspects. 1) It provides one order of magnitude better resolution. 2) It allows simultaneous imaging of the detailed morphology of the tumor and its surrounding microvasculature, which paves the way for further study of tumor metabolism. 3) The concentration of the blue product in the tumor can be quantified. 4) It eliminates the need for registration between images obtained before and after X-gal injection, which could be painful.

Currently, methods for *in-vivo* imaging of lacZ expression are limited. Two approaches have been reported using planar fluorescence imaging²² and magnetic resonance imaging²³, respectively. Compared with them, our method has two advantages. 1) It is capable of simultaneously imaging microvasculature with a 10- μm -order resolution using endogenous contrast. 2) It can potentially provide information about local metabolism *in vivo*, which is of special interest in cancer research.

As we discussed earlier, we noticed limitations of our current strategy, mainly associated with the *in-vivo* use of X-gal¹⁶. A new analyzing assay for lacZ-gene expression or a novel reporter-gene technique is needed, designed specially for photoacoustic imaging. The ideal reporter-gene system would have the following features. 1) The final reporter molecule has strong optical absorption. Its absorption spectrum is preferred to peak in the far-red or near-infrared region of the optical spectrum, where the absorption of major endogenous absorbers is weak. 2) Sufficient accumulation of the absorbing reporter molecules can be achieved following systemic administration of a reasonable dose of reporter probe or analyzing assay. 3) All molecules involved in the system are safe for *in-vivo* application. 4) It can be used to study interesting biology, like gene therapy. We believe this is a promising direction, considering the vast number of naturally occurring pigments in nature.

In conclusion, we can visualize ‘invisible’ tumors using photoacoustic imaging with the help of the reporter-gene technique. Using a new dual-wavelength photoacoustic microscopy, we were able to image the detailed morphology of a lacZ-marked tumor and its surrounding microvasculature simultaneously *in vivo*. With future development of better absorption-enhancing reporter-gene techniques, we expect that our strategy, which combines photoacoustic imaging and the reporter gene technique, can make significant contributions to cancer research.

Acknowledgments

We are grateful to Gina Lingu and Professor George Stoica for assistance with cell cultures and animal handling. This research is funded in part by the NIH grants R01 NS46214 (BRP) and R01 EB000712.

References

1. Jemal A, Siegel R, Ward E, Murray T, Xu J, Thun MJ. Cancer Statistics. *CA Cancer J Clin* 2007;57:43–66. [PubMed: 17237035]
2. Massoud TF, Gambhir SS. Molecular imaging in living subjects: seeing fundamental biological in a new light. *Genes & Development* 2003;17:545–80. [PubMed: 12629038]
3. Weissleder R. Molecular Imaging in Cancer. *Science* 2006;312:1168–1171. [PubMed: 16728630]
4. Herschman, HR.; George, FVW.; George, K. *Advances in Cancer Research*. Academic Press; 2004. Noninvasive Imaging of Reporter Gene Expression in Living Subjects; p. 29-80.
5. Bouvet M, Wang J, Nardin SR, Nassirpour R, Yang M, Baranov E, Jiang P, Moossa AR, Hoffman RM. Real-time optical imaging of primary tumor growth and multiple metastatic events in a pancreatic cancer orthotopic model. *Cancer Res* 2002;62:1534–1540. [PubMed: 11888932]
6. Forss-Petter S, Danielson PE, Catsicas S, Battenberg E, Price J, Nerenberg M, Sutcliffe IG. Transgenic mice expressing beta-galactosidase in mature neurons under neuron-specific enolase promoter control. *Neuron* 1990;5:187–200. [PubMed: 2116814]
7. Steffens S, Frank S, Fischer U, Heuser C, Meyer KL, Dobberstein KU, Rainov NG, Kramm CM. Enhanced green fluorescent protein fusion proteins of herpes simplex virus type 1 thymidine kinase and cytochrome P450 4B1: Applications for prodrug-activating gene therapy. *Cancer Gene Ther* 2000;7:806–812. [PubMed: 10830728]
8. Wang LV. Tutorial on Photoacoustic Microscopy and Computed Tomography. *IEEE Journal of Selected Topics in Quantum Electronics* 2008;14:171–179.
9. Xu M, Wang LV. Photoacoustic imaging in biomedicine. *Review of Scientific Instruments* 2006;77:041101.
10. Wang X, Pang Y, Ku G, Xie X, Stoica G, Wang LV. Non-invasive laser-induced photoacoustic tomography for structural and functional imaging of the brain *in vivo*. *Nat Biotech* 2003;21:803–806.
11. Zhang HF, Maslov K, Stoica G, Wang LV. Functional photoacoustic microscopy for high-resolution and noninvasive *in vivo* imaging. *Nat Biotech* 2006;24:848–851.
12. Ku G, Wang X, Xie X, Stoica G, Wang LV. Imaging of tumor angiogenesis in rat brains *in vivo* by photoacoustic tomography. *App Opt* 2005;44:770–775.

13. Wang X, Xie X, Ku G, Stoica G, Wang LV. Non-invasive imaging of hemoglobin concentration and oxygenation in the rat brain using high-resolution photoacoustic tomography. *J Biomed Opt* 2006;11:024015. [PubMed: 16674205]
14. Zhang HF, Maslov K, Sivaramakrishnan M, Stoica G, Wang LV. Imaging of hemoglobin oxygen saturation variations in single vessels *in vivo* using photoacoustic microscopy. *App Phys Lett* 2007;90:053901.
15. Carmeliet P, Jain RK. Angiogenesis in cancer and other diseases. *Nature* 2000;407:249–257. [PubMed: 11001068]
16. Li L, Zemp R, Lungu G, Stoica G, Wang LV. Photoacoustic imaging of lacZ gene expression *in vivo*. *J Biomed Opt* 2007;12:020504. [PubMed: 17477703]
17. Oh JT, Li ML, Zhang HF, Maslov K, Stoica G, Wang LV. Three-dimensional imaging of skin melanoma *in vivo* by dual-wavelength photoacoustic microscopy. *J Biomed Opt* 2006;11:034032.
18. American national standard for the safe use of lasers Z136.1, (American National Standards Institute, New York, 2000).
19. Li ML, Zhang H, Maslov K, Stoica G, Wang LV. Improved *in-vivo* photoacoustic microscopy based on a virtual detector concept. *Opt Lett* 2006;31:474–476. [PubMed: 16496891]
20. Jacques, SL.; Prahl, SA. Absorption Spectra for Biological Tissues. <http://omlc.ogi.edu/spectra/hemoglobin/index.html>
21. Beumont TL, Kupsky WL, Barger GR, Sloan AE. Gliosarcoma with multiple extracranial metastases: case report and review of the literature. *J Neurooncology* 2007;83:39–46.
22. Tung C, Zeng Q, Shah K, Kim DE, Schellingerhout D, Weissleder R. *In vivo* imaging of β -galactosidase activity using far red fluorescent switch. *Cancer Res* 2004;64:1579–1583. [PubMed: 14996712]
23. Louie AY, Huber MM, Ahrens ET. *In vivo* visualization of gene expression using magnetic resonance imaging. *Nat Biotech* 2000;18:321–325.

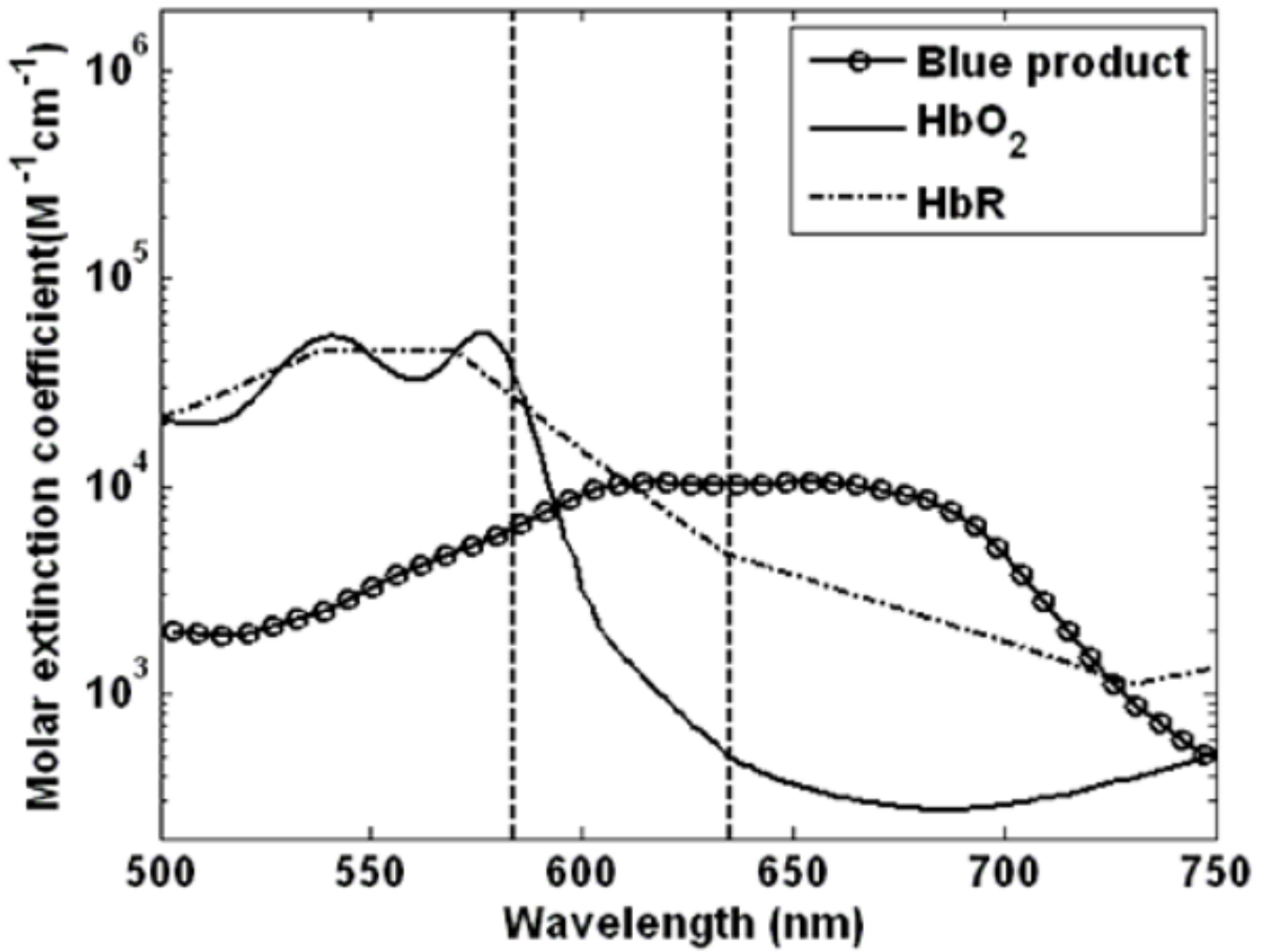


Figure 2.
Comparison of the molar extinction spectra of the blue product, HbO₂, and HbR.

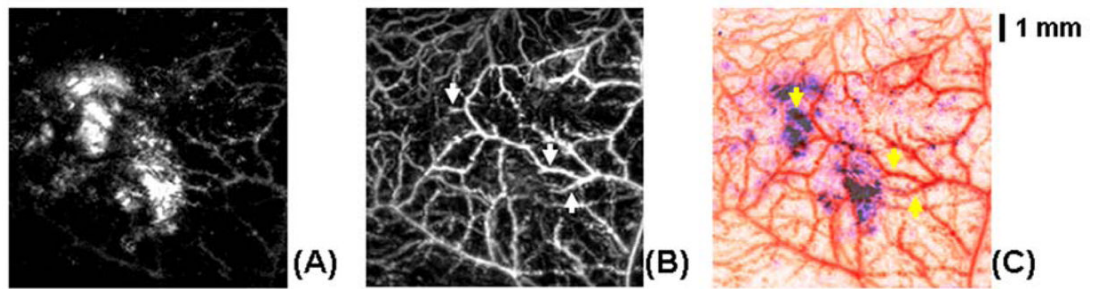


Figure 3.

In-vivo images of lacZ-marked tumor by dual-wavelength photoacoustic microscopy. (A) MAP image acquired at 635 nm showing tumor morphology. (B) MAP image acquired at 584 nm showing microvasculature, or the spatial distribution of total hemoglobin concentration. (C) Combined pseudo-colored image showing the spatial relations between tumor and vascular network. Red: Blood vessels. Blue: tumor. Arrows indicate feeding vessels of tumor.